Vibrational Spectroscopy of the Pyridazine Cation in the Ground State

Kyo-Won Choi, Doo-Sik Ahn, Joo-Hee Lee, and Sang Kyu Kim*

Department of Chemistry and School of Molecular Science (BK21), Korea Advanced Institute of Science and Technology (KAIST), Daejeon 305-701, Republic of Korea

Received: November 11, 2005; In Final Form: December 27, 2005

Vibrational structure of the pyridazine cation in the ground state has been revealed by a vacuum-ultraviolet mass-analyzed threshold ionization (VUV-MATI) spectroscopy. The adiabatic ionization energy is precisely measured to be 70241 ± 6 cm^{-1} (8.7088 ± 0.0007 eV). The origin is very weakly observed, while a long progression of the ν_9^+ (a_1) band of which the fundamental vibrational frequency is 647 cm^{-1} is predominantly observed. The ν_9^+ (a_1) mode progression combined with one quantum of the ν_3^+ (a_1) band at 1698 cm^{-1} is found to be even stronger. Many other weakly observed vibrational features of the pyridazine cation are identified in the vibrational energy of 0−3500 cm^{-1}. The structural change of pyridazine upon ionization, reflected in the vibrational spectrum obtained by the one-photon direct ionization process, is theoretically predicted by ab initio calculations. Ring distortion including contraction of the N═N bond should be responsible for strong excitations of ν_3^+ and ν_9^+ modes. Franck−Condon analysis is given for the comparison of the experiment and theory.

I. Introduction

Photochemistry of diazabenzenes has received a great deal of attention because of intriguing through-bond and through-space interactions of two nonbonding orbitals located at three relatively different positions of the ring in pyrazine, pyrimidine, and pyridazine.[1−6] Excited states of diazabenzenes received special attention in terms of their electronic dephasing mechanisms, molecular structures, and vibronic couplings of excited states.[7−14] Photochemical properties of pyridazine, compared to those of pyrazine and pyrimidine, are relatively less investigated, and many fundamental properties still remain unresolved. For instance, the vibronic structure of the first electronic state of pyridazine has long been in controversy because of the possible presence of a nearby second electronically excited state.[6,7,9,13] Structural distortion of the S_1 pyridazine due to the local excitation or severe vibronic coupling between S_1 and S_2 are two possible scenarios for the explanation of the complex S_1-S_0 vibronic spectral features.[6,13] The lifetime of the pyridazine in the S_1 state has only recently been reported to be ∼320 ps at its origin.[11] A femtosecond photoelectron imaging study has shown that the major dephasing mechanism of the S_1 pyridazine should be internal conversion.[11]

Ionization spectroscopy of diazabenzenes is also of considerable interest, since it provides the relative energy of valence orbitals which should be closely related to orbital interactions among valence electrons. Photoelectron spectroscopy of all three diazabenzenes had been reported to give the relative orbital energies according to Koopmans' theorem.[12,15] Especially, for pyrazine, even distinct vibrational features in carefully measured PES had been reported, though accurate mode assignment was not accomplished due to relatively poor energy resolution of PES.[15] Vibrational spectroscopy of a cation in high resolution provides direct information about the geometrical change which is accompanied by the removal of an electron from a particular orbital. An experimental technique of zero-electron kinetic energy (ZEKE) or mass-analyzed threshold ionization (MATI) spectroscopy is an ideal tool for this purpose.[16] Since ZEKE can provide a spectral resolution of less than 1 cm^{-1}, vibrational structure can be more or less thoroughly investigated. Accordingly, two-color (1 + 1′) ZEKE or MATI spectroscopy of pyrazine,[17] pyrimidine,[18] and pyridazine[13] had already been reported to give vibrational frequencies of their ground cationic states. In two-color (1 + 1′) ZEKE or MATI spectroscopy, the vibrational spectrum of the cation indispensably reflects that of the electronically excited S_1 state which is used as an intermediate state for the ionization. Interference of the intermediate state on the ionization spectrum in some cases could be very useful for investigating the nature of the electronically excited state in terms of mode characterization and anharmonic couplings. Ironically, however, when the intermediate state is not unambiguously characterized in terms of its geometrical structure and mode couplings, it is nontrivial to infer structural information of the cationic state from two-photon ionization spectroscopy. In this occasion, one-photon vacuum-ultraviolet (VUV) ionization spectroscopy would be an ideal tool since the neutral ground-state structure of the molecule is usually firmly established.

In this work, we have applied the VUV-MATI spectroscopic technique for unraveling the vibrational structure of the pyridazine cation. It is found that the one-photon MATI spectrum is totally different from the previously reported two-color (1 + 1′) MATI spectrum,[13] providing direct information about the structural change of pyridazine upon ionization with associated vibrational frequencies. Ab initio calculation has been carried out for the cationic structure of the pyridazine, and Franck−Condon analysis is presented for the explanation of the spectral pattern observed.

II. Experimental Section

Experimental Methods. A supersonic jet of pyridazine was formed by expanding the mixture of pyridazine and Ar into a

* Corresponding author. Fax: (+82) 42-869-2810. E-mail: sangkyukim@kaist.ac.kr.

10.1021/jp056532p CCC: $33.50
Published on Web 02/04/2006

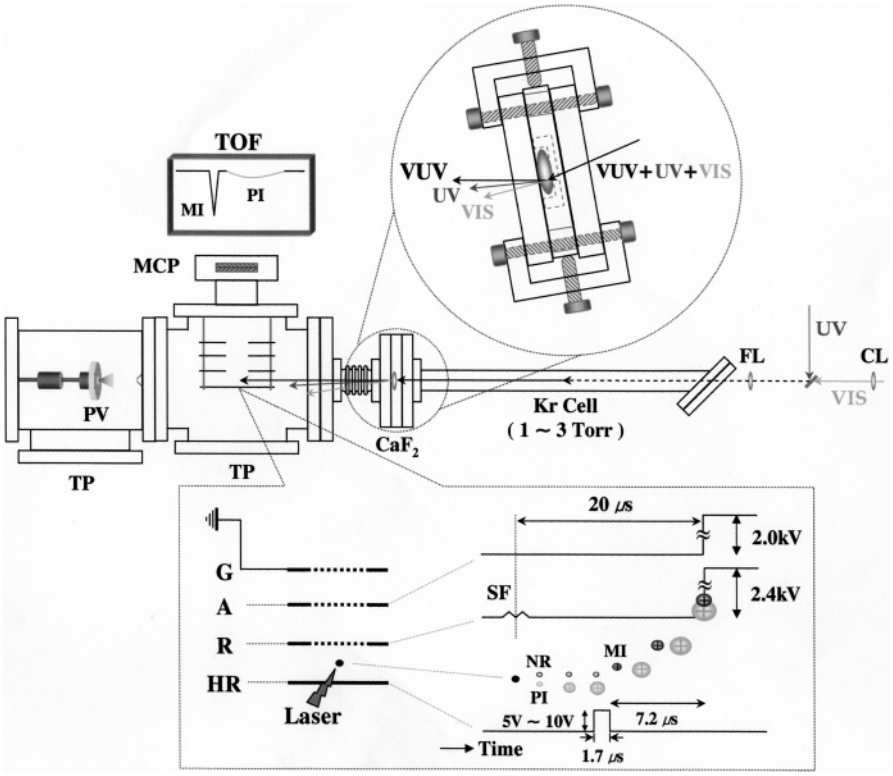

Figure 1. Experimental setup for taking the VUV-MATI spectrum. The VUV laser pulse was separated from UV and VIS fundamentals by tilting a CaF_2 lens on the exit of the four-wave mixing cell. PV: pulsed valve, TP: turbo pump, MCP: microchannel plate, PI: prompt ion, MI: MATI ion, NR: neutral Rydberg, SF: scrambling field, HR: high resolution, R: repeller plate, A: accelerator plate, G: ground, FL: focusing lens, and CL: collimating lens.

vacuum through the nozzle orifice (General valve, 0.5 mm diameter orifice) heated at 100 °C. The backing pressure was 1.2 atm. The molecular beam chamber was differentially pumped with two molecular turbo pumps to maintain the background pressure of 10^{-7} Torr when the nozzle was on. The molecular beam was skimmed through a 1 mm diameter skimmer (Precision Instrument Services) for the collimation of the beam. The third harmonic output of a Nd:YAG laser (Continuum, Precision II) was split into half to pump two independently tunable dye lasers. One dye laser (Lambda-Physik, Scanmate 2) was used for the generation of the UV laser pulse by frequency doubling through a BBO crystal, while the other dye laser (Lumonics, HD-500) was used to generate the tunable visible laser pulse. A VUV laser pulse in the 135−142 nm range was generated via the four-wave mixing process in a Kr cell (1−3 Torr) using the fixed 212.552 nm UV laser pulse for the two-photon Kr $5p[1/2]_0-4p^6$ transition and the tunable visible laser pulse in the 430−492 nm range for the VUV laser frequency tuning. A Xe cell was also used for the generation of VUV laser pulses in the 137−140 nm range using the Xe $6p'[1/2]_0-5p^6$ transition at 222.562 nm. The resultant VUV laser pulse ($\Delta t \sim 5$ ns) was then separated from UV and visible fundamentals using the edge of the collimating CaF_2 lens to be overlapped collinearly with the molecular beam of pyridazine seeded in the Ar carrier gas, as shown in Figure 1. The long-lived high-lying Rydberg states reached by the VUV photon are pulsed-field-ionized after the delay time of 15 μs following the VUV laser pulse to give the MATI signal. No spoil field was necessary for the separation of MATI ions from directly formed ions because of the long time delay between the laser irradiation and pulsed-field ionization. To obtain high-energy resolution, a small electric field of ~8 V/cm was applied for the pulsed-field ionization. Ions generated by the pulsed-field were accelerated, drifted along the time-of-flight axis, and detected by dual microchannel plates. Ion signals were digitized by a digital oscilloscope (LeCroy, LT584M) and stored in a personal computer using a data-taking program which controls the dye laser tuning also.

Computational Methods. All of the ab initio and DFT calculations are implemented with the Gaussian03W set of programs.[19] We carried out various geometry optimizations and normal-mode analysis to find the global minimum structure of the neutral and cationic states of pyridazine. These geometry optimizations and calculations of harmonic frequencies are performed on the Möller−Plesset second-order perturbation theory (MP2)[20] and density functional theory (B3LYP)[21,22] with the aug-CC-pVDZ[23] basis set. All harmonic frequencies reported here are not scaled. Franck−Condon overlap integrals using the Duschinsky transformation[24] are calculated with a code developed by Peluso and co-workers.[25,26] Optimized structures and normal-mode frequencies are used as inputs for both neutral and cationic states.

III. Results and Discussion

The VUV-MATI spectrum of jet-cooled pyridazine taken at 0−3500 cm^{-1} above the ionization threshold is shown in Figure 2. The adiabatic ionization energy is precisely determined to be 70241 ± 6 cm^{-1} after correction for the field effect on the ionization energy. The same correction has been applied to the determination of the ionization energy of pyrazine. According to our correction for the field effect on the MATI signal, the ionization energy of 74906 ± 4 cm^{-1} is obtained, which is consistent with the previously reported value of 74908 cm^{-1} from a ZEKE study of pyrazine by the Johnson group.[17] In Figure 2, surprisingly, the $0-0^+$ origin is found to be extremely weak, while a long progression is predominant for the 647-cm^{-1} band. The progression shows a maximum intensity for

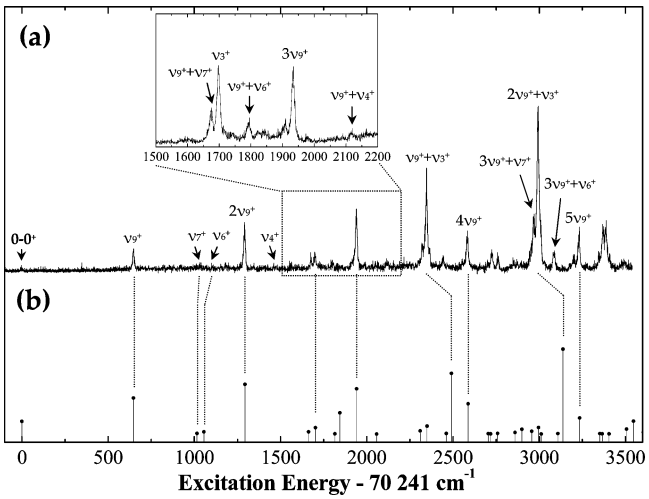

Figure 2. (a) The VUV-MATI spectrum of the pyridazine cation in the vibrational energy region of 0−3500 cm^{-1}. The VUV laser intensity in the 1500−2200 cm^{-1} region from a Kr cell was relatively low due to the decrease of the dye laser efficiency. Thus, a Xe cell was instead used to get a spectrum shown in the inset. (b) The simulated spectrum calculated by Franck−Condon overlap integrals based on ab initio geometries calculated by MP2 (see the text).

TABLE 1: Experimental and Ab Initio Values for Vibrational Frequencies of the Pyridazine Cation

		observed		calculated		
		VUV-MATI[a]	(1 + 1) MATI[b]	DFT[c]	MP2[d]	descriptions[e]
A_1	ν_1^+			3251	3289	$C_{3(6)}H_{3(6)}$ str.
	ν_2^+			3211	3243	$C_{4(5)}H_{4(5)}$ str.
	ν_3^+	1698		1787	1844	N_1N_2 str. + C_4C_5 str.
	ν_4^+	1469		1509	1558	C_4C_5 str.
	ν_5^+			1320	1411	$N_{2(1)}C_{3(6)}$ str. + $C_{3(6)}C_{4(5)}$ str.
	ν_6^+	1151		1164	1168	$C_{4(5)}H_{4(5)}$ rock.
	ν_7^+	1029		1083	1056	$N_{2(1)}C_{3(6)}$ str. + $C_{4(5)}H_{4(5)}$ rock.
	ν_8^+			1043	1016	ring def.
	ν_9^+	647	648	658	647	ring def.
A_2	ν_{10}^+			1014	1029	$C_{4(5)}H_{4(5)}$ wag.
	ν_{11}^+			920	921	$C_{3(6)}H_{3(6)}$ wag.
	ν_{12}^+			658	834	ring tors.
	ν_{13}^+		410[f]	420	435	ring tors.
B_1	ν_{14}^+			978	947	$C_{3(6)}H_{3(6)}$ wag. + $C_{4(5)}H_{4(5)}$ wag.
	ν_{15}^+			770	761	$C_{3(6)}H_{3(6)}$ wag. + $C_{4(5)}H_{4(5)}$ wag.
	ν_{16}^+		369[f]	386	363	ring tors.
B_2	ν_{17}^+			3250	3236	$C_{3(6)}H_{3(6)}$ str.
	ν_{18}^+			3202	3231	$C_{4(5)}H_{4(5)}$ str.
	ν_{19}^+		1476	1498	1515	$N_{2(1)}C_{3(6)}$ str. + $C_{3(6)}C_{4(5)}$ str.
	ν_{20}^+		1363	1399	1361	$N_{2(1)}C_{3(6)}$ str. + $C_{4(5)}H_{4(5)}$ rock.
	ν_{21}^+		1263	1285	1252	$N_{2(1)}C_{3(6)}$ str. + $C_{3(6)}H_{3(6)}$ rock.
	ν_{22}^+		1090	1101	1106	$N_{2(1)}C_{3(6)}$ str. + $C_{3(6)}C_{4(5)}$ str.
	ν_{23}^+		879	893	3583[g]	ring def.
	ν_{24}^+		537	559	741	ring def.

[a] This work. [b] Ref 13. [c] DFT (UB3LYP/aug-CC-pVDZ) not-scaled vibrational frequencies. [d] MP2 (UMP2/aug-CC-pVDZ) not-scaled vibrational frequencies. [e] Normal mode descriptions are based on the inspection of nuclear displacement vectors of each mode (Figure 3); str.: stretching, rock.: rocking, wag.: wagging, def.: deformation, tors.: torsion. [f] Very weak. [g] A normal mode at 3583 cm^{-1} from MP2 includes additional C−H stretching motions.

the second overtone ($\upsilon^+ = 3 \leftarrow \upsilon = 0$) transition. The 647-$cm^{-1}$ band is assigned as the ν_9^+ (a_1) mode from the comparison with ab initio vibrational frequencies of 658 or 647 cm^{-1} from DFT and MP2 calculations, Table 1. It is interesting to note that the ν_9^+ progression band follows a harmonic behavior up to $\upsilon^+ = 5$. The ν_9^+ (a_1) mode is associated with ring-breathing motion as depicted in Figure 3, and this indicates that the structural change of pyridazine upon ionization is quite significant in terms of ring distortion. The ν_9^+ mode progression bands combined with the 1698 cm^{-1} band are found to be even stronger at 2346 and 2992 cm^{-1}. The 1698 cm^{-1} band should correspond to the ν_3^+ (a_1) mode where the N═N bond stretching is mainly involved, Figure 3. The corresponding ab initio frequency is 1787 or 1844 cm^{-1} from DFT and MP2, respectively, Table 1.

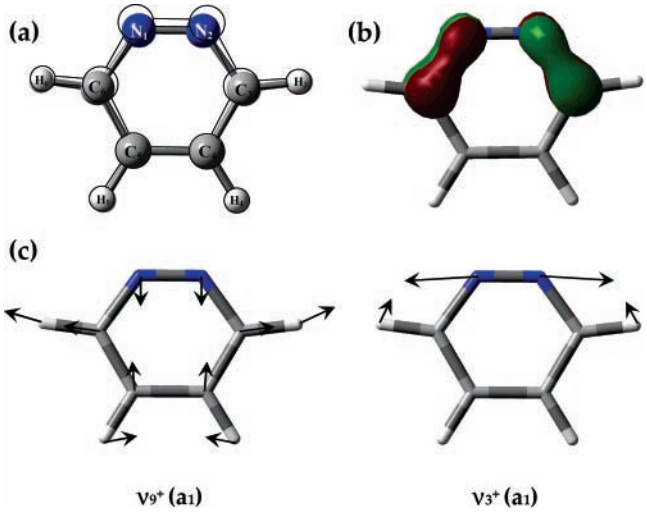

Figure 3. (a) Ab initio (MP2) calculated minimum energy structures of pyridazine in the neutral (circle-and-rod) and cationic (ball-and-stick) ground states. (b) Singly occupied molecular orbital (SOMO) of the pyridazine cation. (c) Normal mode descriptions for ν_9^+ and ν_3^+ modes.

TABLE 2: Structural Parameters of Pyridazine in the Neutral and Cationic Ground States

	neutral ground		cationic ground	
	DFT	MP2	DFT	MP2
bond lengths (Å)				
N_1-N_2	1.334	1.350	1.222	1.228
N_2-C_3	1.338	1.353	1.339	1.362
C_3-C_4	1.400	1.407	1.405	1.400
C_4-C_5	1.386	1.397	1.394	1.414
C_3-H_3	1.091	1.094	1.088	1.090
C_4-H_4	1.090	1.093	1.091	1.094
bond angles (°)				
$N_1-N_2-C_3$	119.5	119.1	125.5	125.4
$N_2-C_3-C_4$	123.6	124.1	115.1	114.8
$C_3-C_4-C_5$	116.9	116.8	119.4	119.8
$N_2-C_3-H_3$	115.0	114.5	118.8	118.0
$C_3-C_4-H_4$	120.9	120.9	119.0	119.1

The experimental finding that the ν_9^+ and ν_3^+ modes are strongly enhanced in the VUV-MATI spectrum obviously indicates that pyridazine undergoes a large structural change upon ionization. We carried out ab initio calculations to obtain the structure of the pyridazine cation in its minimum energy. As expected from the spectrum, the calculated minimum energy structure of the pyridazine cation is much distorted from that of the neutral ground-state pyridazine, Figure 3. For example, upon ionization, the N═N bond becomes shortened to 1.228 Å from 1.350 Å in the neutral ground state. In addition, the N−C−C angle decreases from 124.1° to 114.8°, Table 2. The origin for the large structural change upon ionization can be found by inspection of the singly occupied molecular orbital (SOMO) of the cation. Although the electron is removed from the nonbonding orbital of the neutral pyridazine, ultrafast electronic rearrangement in the ionization process results in the electron deficiency in the π_3 orbital which has antibonding character along the N−N bond, as depicted in Figure 3b. In the one-photon MATI spectrum where the neutral ground state is

TABLE 3: Observed Vibration Frequencies with Assignments[a]

	$+n\nu_9^+$							
	$n=0$	$n=1$	$n=2$	$n=3$	$n=4$	$+\nu_7^+$	$+\nu_3^+$	$+\nu_7^+ + \nu_3^+$
ν_9^+	647	1292	1939	2583	3232	1676	2346	3370
ν_7^+	1029	1676	2322	2968			2725	
ν_6^+	1151	1798	2443	3086				
ν_4^+	1469	2116	2761	3409				
ν_3^+	1698	2346	2992			2725	3385	

[a] Values in each row are those of progression or combination bands built on the mode shown in the first column.

directly ionized, vibronic bands with large Franck−Condon overlaps should be strongly observed. Accordingly, the Franck−Condon calculation based on the ab initio molecular structures is carried out for the explanation of the experiment. Minimum energy structures and normal mode displacement vectors of neutral and cationic ground states are given as inputs. Minimum energy structures of the pyridazine cation calculated by DFT and MP2 are described in Table 2. Squares of Franck−Condon overlap integrals, plotted in Figure 2, explain the experiment quite successfully. As expected, Franck−Condon integrals for the ν_9^+ mode progression bands are calculated to be large, which is consistent with the experiment. The strongly observed ν_3^+ mode at 1698 cm^{-1} and its combination bands associated with ν_9^+ are also well reproduced by the Franck−Condon analysis.

According to calculations, the molecule retains its C_{2v} symmetry and planarity upon ionization, and thus only totally symmetric vibration modes are expected to have strong signal intensities. Namely, though all vibrational modes of the cation are symmetry-allowed because of flexible symmetries of a departing electron wave function, only totally symmetric vibrational wave functions of the cationic pyridazine, within Born−Oppenheimer approximation, are expected to have considerable overlaps with the totally symmetric neutral ground zero-point vibrational wave function. This is totally consistent with the observation. Other relatively weak bands are appropriately assigned with the help of the ν_9^+ progression intensity pattern. The 1676 cm^{-1} band, for instance, is most likely to be a combination band of ν_9^+ and 1029 cm^{-1} which is calculated from a simple algebra of $1029 = 1676 - 647$. The 1029 cm^{-1} fundamental band is very weak in its intensity and just barely identified in the spectrum. Assignments for the ν_9^+ progression bands combined with 1029 cm^{-1} are then quite straightforward. This band correlates to the ab intio value of 1083 or 1056 cm^{-1} from DFT and MP2, respectively, and assigned as ν_7^+ (a_1), Table 1. Franck−Condon analysis for this mode predicts reasonable intensities for these bands, Figure 2. Vibrational bands observed at 1798, 2443, and 3068 cm^{-1} should be another ν_9^+ progression bands combined with a fundamental band at $(1798 - 647 =)$ 1151 cm^{-1}, which is assigned as the ν_6^+ (a_1) mode of which the ab initio value is 1164 or 1168 cm^{-1} from DFT and MP2, respectively, Table 1. Franck−Condon overlap integrals for $\nu_6^+ + n\nu_9^+$ progression bands also predict the experiment quite well as shown in Figure 2. Weakly observed bands at 2116, 2761, and 3409 cm^{-1} are assigned as ν_9^+ progression bands built on a ν_4^+ fundamental band at $(2116 - 647 =)$ 1469 cm^{-1}, which correlates to 1509 or 1558 cm^{-1} from DFT or MP2, respectively. Other weakly observed bands are also tentatively assigned. Observed frequencies with appropriate assignments are given in Table 3.

It is very interesting to note that vibrational bands identified in the one-photon VUV-MATI spectrum in this work are so different from those found in the $(1 + 1')$ two-color MATI spectrum reported in ref 13 in terms of mode identities and intensities. In the $(1 + 1')$ two-color two-photon MATI spectra taken via various intermediate states, a number of b_2 vibrational modes in C_{2v} have been identified. On the other hand, only totally symmetric modes are strongly observed in the one-photon VUV-MATI spectrum. This fact strongly indicates that the S_1 state which has been used as an intermediate state in the two-photon ionization process may adopt the minimum energy structure which is planar but asymmetrically distorted with respect to the C_2 axis. Vibrational modes associated with asymmetric ring distortion on the plane of molecule are then Franck−Condon-active in both S_1-S_0 and D_0-S_1 transitions to give strong intensities for b_2 vibrational modes in C_{2v}. In other words, the symmetry of pyridazine may be lowered to C_S in the S_1 state while the structure of pyridazine belongs to C_{2v} in both neutral and cationic ground states. In the molecular orbital (MO) picture, the highest-occupied molecular orbital (HOMO) of pyridazine should be the nonbonding orbital (n_-) of which the nature is mainly the mixture of two adjacent atomic orbitals of nitrogen atoms in the ring. Therefore, the adiabatic ionization energy of 8.7088 eV determined in this work, within the Koopmans' approximation, should represent the orbital energy of n_-. Electronic rearrangement after the molecular ionization should be responsible for the accompanying structural change. Efficient electron delocalization after the molecular ionization should be responsible for the maintenance of C_{2v} symmetry in the minimum energy structure of the pyridazine cation.

IV. Summary and Conclusions

In this work, one-photon VUV-MATI spectroscopy is carried out for unraveling the vibrational structure of the pyridazine cation in its ground state. Adiabatic ionization energy is accurately determined to give 8.7088 eV, and this should approximately correspond to the orbital energy of n_-. The $0-0^+$ origin is found to be extremely weak, while the progression bands due to the ν_9^+ mode is dominantly observed. The ν_9^+ progression bands combined with the 1698 cm^{-1} band are even stronger. Franck−Condon analyses based on the molecular structures and vibrational frequencies calculated by ab initio methods (DFT and MP2) are very successful in explaining most of spectral features in the VUV-MATI spectrum. Both experiment and theory indicate that the pyrazine cation adopts a symmetrically distorted planar structure which belongs to C_{2v} symmetry. Efficient electron delocalization after the removal of an electron from the n_- orbital should be responsible for the C_{2v} structure of the pyridazine cation. Comparison of this work with the $(1 + 1')$ two-color two-photon MATI spectrum which was reported previously may suggest that the S_1 pyridazine adopts the C_S structure at the minimum energy.

Acknowledgment. This work was supported by the Korea Science and Engineering Foundation (No. R01-2005-000-10117-0).

References and Notes

(1) Hoffman, R. *Acc. Chem. Res.* **1971**, *4*, 1, and references therein.
(2) Innes, K. K.; Ross, I. G.; Moomaw, W. R. *J. Mol. Spectrosc.* **1988**, *132*, 492.
(3) Fülscher, M. P.; Andersson, K.; Roos, B. O. *J. Phys. Chem.* **1992**, *96*, 9204.
(4) Kleier, D. A.; Martin, R. L.; Wadt, W. R.; Moomaw, W. R. *J. Am. Chem. Soc.* **1982**, *104*, 60.
(5) Wadt, W. R.; Goddard, W. A., III, *J. Am. Chem. Soc.* **1975**, *97*, 2034.
(6) Fischer, G.; Wormell, P. *Chem. Phys.* **2000**, *257*, 1, and references therein.

(7) Terazima, M.; Yamauchi, S.; Hirota, N.; Kitao, O.; Nakatsuji, H. *Chem. Phys.* **1986**, *107*, 81.
(8) Li, H.; Kong, W. *J. Chem. Phys.* **1998**, *109*, 4782.
(9) Ueda, E.; Udagawa, Y.; Ito, M. *Chem. Lett.* **1981**, 873.
(10) Knight, A. E. W.; Parmenter, C. S. *Chem. Phys.* **1976**, *15*, 85.
(11) Matsumoto, Y.; Kim, S. K.; Suzuki, T. *J. Chem. Phys.* **2003**, *119*, 300.
(12) Palmer, M. H.; Walker, I. C. *Chem. Phys.* **1991**, *157*, 187.
(13) Choi, K.-W.; Ahn, D.-S.; Lee, S.; Choi, H.; Baeck, K.-K.; Heo, S.-U.; Baek, S. J.; Choi, Y. S.; Kim, S. K. *ChemPhysChem.* **2004**, *5*, 737.
(14) Hillenbrand, S.; Zhu, L.; Johnson, P. *J. Chem. Phys.* **1991**, *95*, 2237.
(15) Åsbrink, E.; Lindholm, E.; Edqvist, O. *Chem. Phys. Lett.* **1970**, *5*, 609.
(16) Müller-Dethlefs, K.; Schlag, E. W. *Annu. Rev. Phys. Chem.* **1991**, *42*, 109.
(17) Zhu, L.; Johnson, P. *J. Chem. Phys.* **1993**, *99*, 2322.
(18) Sato, S.-I.; Omiya, K.; Kimura, K. *J. Electron Spectrosc. Relat. Phenom.* **1998**, *97*, 121.
(19) Frisch, M. J.; Trucks, G. W.; Schlegel, H. B.; Scuseria, G. E.; Robb, M. A.; Cheeseman, J. R.; Montgomery, J. A., Jr.; Vreven, T.; Kudin, K. N.; Burant, J. C.; Millam, J. M.; Iyengar, S. S.; Tomasi, J.; Barone, V.; Mennucci, B.; Cossi, M.; Scalmani, G.; Rega, N.; Petersson, G. A.; Nakatsuji, H.; Hada, M.; Ehara, M.; Toyota, K.; Fukuda, R.; Hasegawa, J.; Ishida, M.; Nakajima, T.; Honda, Y.; Kitao, O.; Nakai, H.; Klene, M.; Li, X.; Knox, J. E.; Hratchian, H. P.; Cross, J. B.; Bakken, V.; Adamo, C.; Jaramillo, J.; Gomperts, R.; Stratmann, R. E.; Yazyev, O.; Austin, A. J.; Cammi, R.; Pomelli, C.; Ochterski, J. W.; Ayala, P. Y.; Morokuma, K.; Voth, G. A.; Salvador, P.; Dannenberg, J. J.; Zakrzewski, V. G.; Dapprich, S.; Daniels, A. D.; Strain, M. C.; Farkas, O.; Malick, D. K.; Rabuck, A. D.; Raghavachari, K.; Foresman, J. B.; Ortiz, J. V.; Cui, Q.; Baboul, A. G.; Clifford, S.; Cioslowski, J.; Stefanov, B. B.; Liu, G.; Liashenko, A.; Piskorz, P.; Komaromi, I.; Martin, R. L.; Fox, D. J.; Keith, T.; Al-Laham, M. A.; Peng, C. Y.; Nanayakkara, A.; Challacombe, M.; Gill, P. M. W.; Johnson, B.; Chen, W.; Wong, M. W.; Gonzalez, C.; Pople, J. A. *Gaussian 03*, revision B.02; Gaussian, Inc.: Pittsburgh, PA, 2003.
(20) Möller, C.; Plesset, M. S. *Phys. Rev.* **1934**, *46*, 618.
(21) Becke, A. D. *J. Chem. Phys.* **1993**, *98*, 5648.
(22) Lee, C.; Yang, W.; Parr, R. G. *Phys. Rev. B* **1988**, *37*, 785.
(23) Dunning, T. H., Jr. *J. Chem. Phys.* **1989**, *90*, 1007.
(24) Duschinsky, F. *Acta Physicochim.* USSR **1937**, 7, 551.
(25) Peluso, A.; Santoro, F.; Re, G. D. *Int. J. Quantum Chem.* **1997**, *63*, 233.
(26) Borrelli, R.; Peluso, A. *J. Chem. Phys.* **2003**, *119*, 8437.